materials

Article

Forced Magnetostrictions and Magnetizations of $Ni_{2+x}MnGa_{1-x}$ at Its Curie Temperature

Takuo Sakon [1,*], Yuhi Hayashi [1], Dexin Li [2], Fuminori Honda [2], Gendo Oomi [3], Yasuo Narumi [4], Masayuki Hagiwara [4], Takeshi Kanomata [5] and Tetsujiro Eto [3]

1. Department of Mechanical and System Engineering, Faculty of Science and Technology, Ryukoku University, Otsu, Shiga 520-2194, Japan; t150289@mail.ryukoku.ac.jp
2. Institute for Materials Research, Tohoku University, Oarai, Ibaraki 311-1313, Japan; dxli@imr.tohoku.ac.jp (D.L.); honda@imr.tohoku.ac.jp (F.H.)
3. Kurume Institute of Technology, Kurume, Fukuoka 830-0052, Japan; geomi@kurume-it.ac.jp (G.O.); teto@kurume-it.ac.jp (T.E.)
4. Center for Advanced High Magnetic Field Science, Graduate School of Science, Osaka University, 1-1 Machikaneyama, Toyonaka, Osaka 560-0043, Japan; narumi@ahmf.sci.osaka-u.ac.jp (Y.N.); hagiwara@ahmf.sci.osaka-u.ac.jp (M.H.)
5. Research Institute for Engineering and Technology, Tohoku Gakuin University, Tagajo, Miyagi 985-8537, Japan; kanomata@mail.tohoku-gakuin.ac.jp

* Correspondence: sakon@rins.ryukoku.ac.jp; Tel.: +81-77-543-7443

Received: 16 September 2018; Accepted: 25 October 2018; Published: 28 October 2018

Abstract: Experimental investigations into the field dependence of magnetization and the relationship between magnetization and magnetostriction in $Ni_{2+x}MnGa_{1-x}$ (x = 0.00, 0.02, 0.04) alloy ferromagnets were performed following the self-consistent renormalization (SCR) spin fluctuation theory of itinerant ferromagnetism. In this study, we investigated the magnetization of and magnetostriction on $Ni_{2+x}MnGa_{1-x}$ (x = 0.02, 0.04) to check whether these relations held when the ratio of Ni to Ga and, the valence electron concentration per atom, e/a were varied. When the ratio of Ni to Ga was varied, e/a increased with increasing x. The magnetization results for x = 0.02 (e/a = 7.535) and 0.04 (e/a = 7.570) suggest that the critical index δ of $H \propto M^{\delta}$ is around 5.0 at the Curie temperature T_C, which is the critical temperature of the ferromagnetic–paramagnetic transition. This result confirms Takahashi's spin fluctuation theory and the experimental results of Ni_2MnGa. The spontaneous magnetization p_S slightly decreased with increasing x. For x = 0.00, the spin fluctuation parameter in k-space (momentum space; T_A) and that in energy space (T_0) were obtained. The relationship between p_{eff}/p_S and T_C/T_0 can also be explained by Takahashi's theory, where p_{eff} indicates the effective magnetic moments. We created a generalized Rhodes-Wohlfarth plot of p_{eff}/p_S versus T_C/T_0 for other ferromagnets. The plot indicates that the relationship between p_{eff}/p_S and T_0/T_C follows Takahashi's theory. We also measured the magnetostriction for $Ni_{2+x}MnGa_{1-x}$ (x = 0.02, 0.04). As a result, at T_C, the plot of the magnetostriction ($\Delta L/L$) versus M^4 shows proportionality and crosses the origin. These magnetization and magnetostriction results were analyzed in terms of Takahashi's SCR spin fluctuation theory. We investigated the magnetostriction at the premartensite phase, which is the precursor state to the martensitic transition. In Ni_2MnGa system alloys, the maximum value of magnetostriction is almost proportional to the e/a.

Keywords: ferromagnetic Heusler alloy; magnetization; magnetostriction; itinerant electron magnetism; premartensite phase

1. Introduction

Spin fluctuation theories have advanced the attempts to elucidate the physical principles of the itinerant electron system [1–5]. According to the self-consistent renormalization (SCR) spin fluctuation theory [1], the external magnetic field H is proportional to the third power of the magnetization M^3 at the Curie temperature T_C. This relation was derived by only considering the transverse modes of the thermal spin fluctuations with respect to the direction of the static and uniform magnetic moment [6,7]. Takahashi proposed SCR theory according to zero-point spin fluctuations, which assimilate both the transverse and the longitudinal components of the fluctuations [3–5,8]. An outstanding characteristic of this theory is the magnetization at T_C. This theory proposed by Takahashi indicates that H is proportional to M^5 at T_C.

The thermo-dynamical relationship between the magnetization M and the external magnetic field H can be expressed by the equation:

$$H = \frac{\partial F}{\partial M} = a(T)M + b(T)M^3 + c(T)M^5 + \cdots \quad (1)$$

where F indicates the spin fluctuation free energy. This appears as Equation (2.59) in Takahashi [8].

As $T \to T_C$, the magnetic susceptibility $\chi(T)$ comes infinite. Therefore,

$$\lim_{T \to T_C} a(T) = \lim_{T \to T_C} \frac{H}{M} = \lim_{T \to T_C} \frac{1}{\chi} = 0 \quad (2)$$

Then, the first expansion coefficient at T_C is $a(T_C) = 0$.

According to the Rhodes-Wohlfarth theory [9], the third expansion coefficient $b(T)$ in Equation (1) remains finite at $T = T_C$. Therefore, the following formula is satisfied at T_C:

$$H = b(T_C)M^3 + c(T_C)M^5 + \cdots \quad (3)$$

Under the Takahashi theory, $b(T)$ vanishes at T_C, as shown in Equation (3.51) in Takahashi [8].

As a result, the M dependence of the magnetic fields H can be explained by the equation:

$$H = c(T_C)M^5 \quad (4)$$

In Equation (4), higher terms are ignored because their magnitudes are smaller than that of the third term. In conclusion, an $H \propto M^5$ relation was obtained.

MnSi [3], CoS_2 [10], $Fe_xCo_{1-x}Si$ [11], and Ni [12] follow the relationship provided in Equation (4). The Heusler isotropic ferromagnetic alloy Ni_2MnGa also follows this relation in a cubic austenite phase [12]. For Ni_2MnGa, the critical index δ of $H \propto M^\delta$ at T_C is δ 4.70 ± 0.5 [12,13].

Takahashi proposed that magnetostriction can be observed due to the itinerant spin fluctuations around T_C [8] because the magnetostriction is calculated from the spin fluctuation free energy. The relationship between the magnetostriction and the magnetization at T_C [8] in Equation (6.101) was explained using the formula

$$\frac{\omega_h(\sigma, t_C)}{\omega_0} = K \times A(0, t_C) \times \frac{\sigma^4}{\sigma_0^4} \quad (5)$$

where t_C is a relative Curie temperature; σ and σ_0 are the magnetization in a magnetic field and the spontaneous magnetization, respectively; ω_0 is the nonmagnetic volume contribution; $w_h(\sigma, t_C)$ is the relative magnetic volume-striction at T_C; K has a constant value in an isothermal state; and $A(0, t_C)$ indicates the amplitude of the thermal spin fluctuations at T_C. Equation (5) indicates that the magnetostriction is proportional to M^4 at T_C. Kittel mentioned that the volume strain $\Delta V/V$ is three times the value of $\Delta L/L$ [14]. Accordingly, volume magnetostriction ($\Delta V/V$) discussions were applied to the results of the magnetostriction $\Delta L/L$ in this experimental study.

For quondam research, an investigation into MnSi, which is famed for its weak itinerant magnetism, was completed [15]. The magnetostriction $\Delta L/L$ versus the square of the magnetization M^2 was analyzed. Around T_C = 30 K, the plot strayed from linearity. Takahashi proposed that around T_C, the magnetostriction is not proportional to the square of the magnetization. $\Delta L/L$ is proportional to M^4 through the origin at T = 29 K around T_C [8]. In a previous study, we investigated the magnetostriction property of a polycrystalline Ni_2MnGa alloy using the self-consistent renormalization (SCR) theory of itinerant ferromagnets [13]. The magnetostriction was found to be proportional to the fourth power of magnetization. At the Curie temperature, magnetostriction crossed the point of origin. These results are in line with Takahashi's spin fluctuation theory. In this study, we investigated $Ni_{2+x}MnGa_{1-x}$ (x = 0.02, 0.04) alloys and studied the effect of varying alloy composition (ratio of Ni and Ga atoms) on magnetostriction. We found that the valence electron concentration per atom, i.e., the ratio e/a, increases with increasing x. The e/a values were 7.50, 7.535, and 7.570 for x = 0.00, 0.02, and 0.04, respectively. The spin fluctuation parameter in wave number space (momentum space) T_A and that in energy space T_0 were obtained from the results of the magnetization measurement. We discuss the relation between p_{eff}/p_S and T_C/T_0 compared with that shown in other itinerant ferromagnets by means of a generalized Rhodes-Wohlfarth plot [8]. We also investigated the e/a dependences of the maximum magnetostriction around the premartensitic–austenitic transition for Ni_2MnGa-type alloys. Researchers have studied the correlation between magnetostriction and the valence electron concentration e/a, which is related to the energy of the electron system [16–18]. In our prior study, we measured the properties of $Ni_2Mn_{1-x}Cr_xGa$ [16]. In these alloys, the e/a was smaller than 7.50, which is the value for Ni_2MnGa. In this study, we measured $Ni_{2+x}MnGa_{1-x}$ (x = 0.02, 0.04) alloys for which the e/a is larger than 7.50 and investigated the e/a dependence of the maximum magnetostriction in the premartensite phase.

Rizal et al. investigated the magnetic property of nanostructured Fe-Co alloys [19]. At room temperature, a strong correlation was found between the saturated magnetization and the lattice constant of the Fe-Co alloy. For Ni_2MnGa-type Heusler alloys, the correlations between e/a and the magnetization (magnetic moment) or magnetostriction have been the subject of several investigations undertaken by varying alloy composition. Accordingly, in this article, we focused on the e/a dependences of the magnetostrictions.

2. Materials and Methods

The polycrystalline samples of $Ni_{2+x}MnGa_{1-x}$ (x = 0.00, 0.02, 0.04) were prepared by arc melting the constituent elements—4N Ni, 3N Mn, and 6N Ga—several times in an Ar atmosphere. Each ingot was melted several times in order to ensure good homogeneity. The products from the arc melting process were sealed in an evacuated silica tube and solution heat-treatments were applied at 1123 K for three days. After these treatments, the sample was quenched in water. The measurement of permeability was performed in alternating current (AC) magnetic fields with a frequency of 73 Hz and a maximum field of $\pm$10 Oe. The AC magnetic fields were measured using a gaussmeter 410 (Lakeshore Cryotronix Inc., Westerville, OH, USA). The sample size chosen for the experimental investigations was 3.0 $\times$ 3.0 $\times$ 4.0 mm. The magnetostriction was measured by means of a strain gauge [13]. The magnetostriction $\Delta L/L$ was measured parallel to the external magnetic field H—the same approach used in the experimental investigation of MnSi [15]. A helium-free superconducting magnet at the Center for Advanced High Magnetic Field Science, Osaka University, Japan was used for the magnetostriction measurements up to 5 T.

The magnetization measurements were performed using a solenoid-type pulsed-field magnet at Ryukoku University, Japan [13]. The absolute value of the magnetization was calibrated with the use of a sample of pure Ni of the same size. The same bulk sample was used in the permeability, magnetization, and magnetostriction measurements in order to compare the results. The data for magnetostriction and magnetization were the results of measurements with increasing magnetic fields beginning with a zero field.

We also used a water-cooled magnet in a steady field up to 1.6 T, which was installed in Ryukoku University, and studied the magnetostriction in order to investigate the temperature dependence of the magnetostriction around the premartensite phase.

3. Results and Discussions

3.1. Magnetic Field Dependence of the Magnetization

For the Ni_2MnGa alloy, martensitic transitions occurred at the temperature T_{MS} of 195 K [16]. The alloy Ni_2MnGa also has a premartensite phase. This is a precursor (intermediate) state to the martensitic transition. In the premartensite phase, the alloy has a 3M modulated structure [20]. The austenitic–premartensitic transition occurs at the premartensitic temperature T_P of 260 K. Above T_P, a cubic $L2_1$ type austenite phase is realized. The Curie temperature T_C is 375 K, which is much higher than T_{MS} and T_P. The ferromagnetic–paramagnetic transition at T_C occurs in the cubic austenite phase, and the magnetic anisotropy constant K_1 in the austenite phase is 1/10 smaller than that in the martensite phase. The K_1 value at 150 K in the martensite phase was of the magnitude 4.0×10^6 erg/cm^3, and K_1 at 293 K in the austenite phase was 0.30×10^6 erg/cm^3 [16]. The magnitude of K_1 of Ni_2MnGa in the austenite phase is comparable to that of Fe. Therefore, Ni_2MnGa was decided to be an isotropic ferromagnet in the austenite phase. The value of T_M for $Ni_{2+x}MnGa_{1-x}$ increased with increasing Ni concentration x. The value of T_P also increased with increasing x for $x \leq 0.04$. Above T_P = 265 K for x = 0.02 and 275 K for x = 0.04, a cubic $L2_1$ type austenite phase is realized. Figure 1 plots the permeability μ for x = 0.02 (Figure 1a) and x = 0.04 (Figure 1b) during heating in a zero external magnetic field. The derivative of μ with respect to temperature, $d\mu/dT$, is also shown in Figure 1. The T_C could not be defined from the μ-T curve because the divergence derived from Equation (2) was not found. Therefore the T_C was defined as a temperature where the absolute value of the gradient of the μ-T curve, $d\mu/dT$ is maximum. The Curie temperatures T_C were found to be 372 K and 366 K for x = 0.02 and 0.04, respectively, as obtained from the peaks of $d\mu/dT$ in Figure 1.

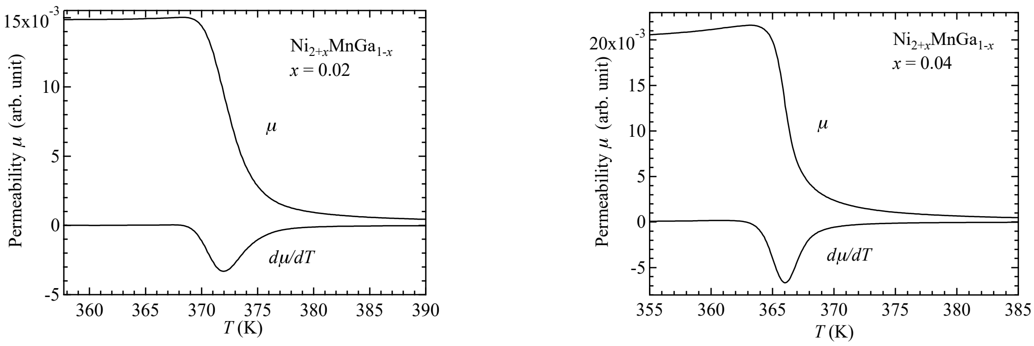

(**a**) (**b**)

Figure 1. Plots of μ vs. T and $d\mu/dT$ vs. T for (**a**) x = 0.02 and (**b**) x = 0.04.

We measured the magnetization of $Ni_{2+x}MnGa_{1-x}$ around T_C for the purpose of ascertaining the critical index δ of $M^{\delta-1}$ versus H/M. We plotted figures of $M^{\delta-1}$ versus H/M for δ = 3.0, 4.7, and 5.0; these are shown in Figures 2–4, respectively. The result for δ = 3 is comparable to Moriya's theory [1], that for δ = 5 is comparable to Takahashi's theory [8], and that for δ = 4.7 is comparable to the former result [12]. $M^{\delta-1}$ versus H/M with δ = 4.7 in Figure 3 and δ = 5.0 in Figure 4 show good linearity through the origin at T_C, denoted by the filled circles. The results suggest that for x = 0.02 and 0.04, the critical index δ is 4.7–5.0, which conforms to Takahashi's theory [8] and the result found for Ni_2MnGa [12,13]. These relations held when the ratio of Ni to Ga and e/a were varied. $H \propto M^5$ behavior was also observed for MnSi [21] and Fe [22]. Therefore, Takahashi's theory was again shown to be acceptable for use in analyzing magnetization in terms of itinerant electron ferromagnetism in Ni_2MnGa system alloys.

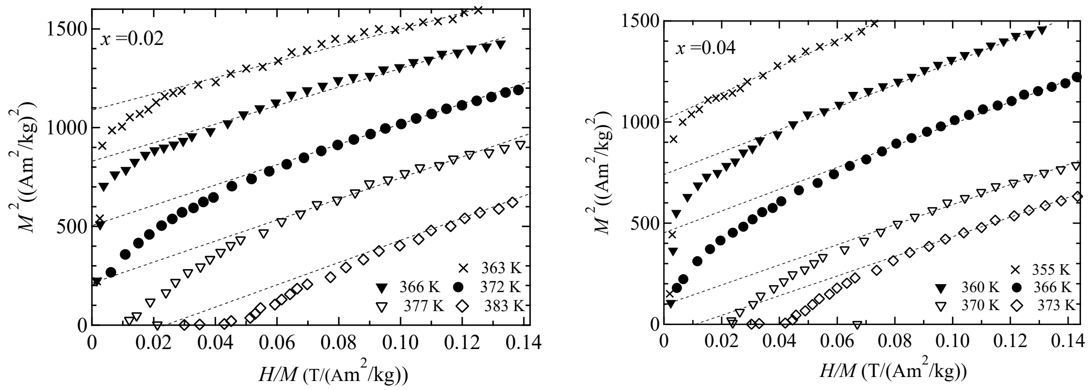

(**a**) (**b**)

Figure 2. The H/M dependences of M^2 for (**a**) x = 0.02 and (**b**) x = 0.04. The dotted straight lines are included as a visual guide.

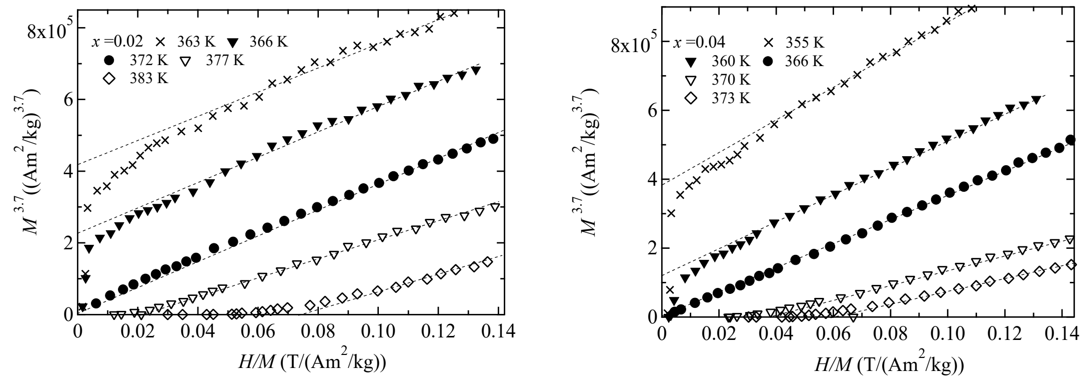

(**a**) (**b**)

Figure 3. The H/M dependences of $M^{3.7}$ for (**a**) x = 0.02 and (**b**) x = 0.04. The dotted straight lines are included as a visual guide.

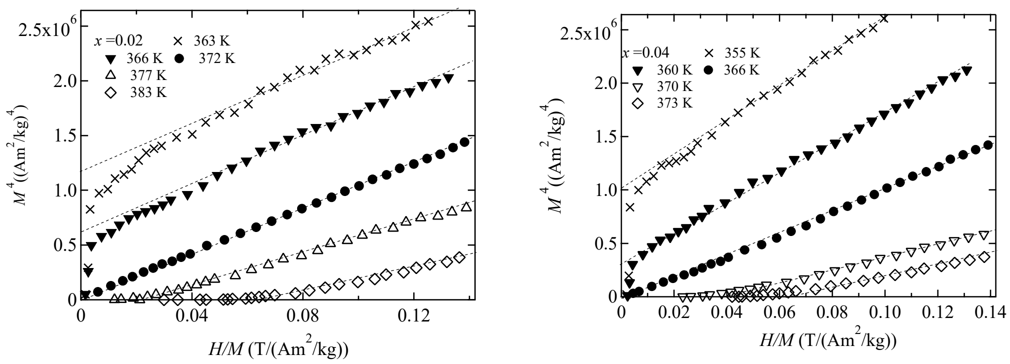

(**a**) (**b**)

Figure 4. The H/M dependences of M^4 for (**a**) x = 0.02 and (**b**) x = 0.04. The dotted straight lines are included as a visual guide.

3.2. Basic Magnetic and Itinerant Spin Fluctuation Parameters and Generalized Rhodes–Wohlfarth Plot

In this subsection, we obtain the basic and spin fluctuation parameters and discuss itinerant magnetism by means of a generalized Rhodes-Wohlfarth plot of $p_{\mathrm{eff}}/p_{\mathrm{S}}$ versus T_{C}/T_0.

The induced magnetization M [8] (Equation (3.61)) is written as:

$$\left(\frac{M}{M_S}\right)^4 = 1.20 \times 10^6 \times \frac{T_C^2}{T_A^3} \times \frac{H}{M} \tag{6}$$

where $M_S = N_0 p_S \mu_B$ represents a spontaneous magnetization in a ground state; N_0 is a molecular number; $p_S = gS$, where g is the Landé's g-factor and S is spin angular momentum; and T_A is the spin fluctuation parameter in wave number space (momentum space). T_A was obtained when experimental values were inserted into Equation (6), where the magnetic field H is in units of kOe and the magnetization M is in units of Am^2/kg, which is equal to emu/g.

The spontaneous magnetic moment p_S (μ_B) is expressed as:

$$p_S^2 = \frac{20T_0}{T_A} \times C_{\frac{4}{3}} \times \left(\frac{T_C}{T_0}\right)^{\frac{4}{3}} C_{\frac{4}{3}} = 1.006089\cdots \tag{7}$$

where T_0 is the width of the spin fluctuation spectrum in the energy scale. This appears as Equation (3.61) in Takahashi [8].

From Equation (7), T_0 can be obtained using the formula:

$$T_0 = \frac{8147.2 \times T_C^4}{T_A^3 \times p_S^6} \tag{8}$$

Table 1 provides the measured spontaneous magnetic moment p_S and the characteristic temperatures T_C, calculated T_A, and T_0 for $Ni_{2+x}MnGa_{1-x}$. As for Ni_2MnGa, the measured p_S of 3.93 μ_B is comparable to the theoretical band calculation result at the experimental lattice constant of the $L2_1$ cubic austenite phase, p_S, at 3.94 μ_B [23]. With increasing Ni fraction, the p_S value decreased. This behavior appears for $Ni_{2+x}Mn_{1-x}Ga$ [24] and Ni_xFe_{1-x} Invar alloys [25]. T_0 increased with increasing x. This is presumably because, in Equation (8), the right side varies with the sixth power of p_S, so T_0 varies even when T_A does not change.

Table 1. The spontaneous magnetic moment p_S and the characteristic temperatures T_C, T_A, and T_0 for $Ni_{2+x}MnGa_{1-x}$.

x	p_S (μ_B)	T_C (K)	T_A (K)	T_0 (K)
0.00	3.93	375	563	245
0.02	3.79	372	566	288
0.04	3.64	366	567	345

Takahashi also derived a formula [8], shown in Equation (3.47), for the relationship between p_S, T_C, T_0, and the effective magnetic moment p_{eff} as follows:

$$\frac{p_{eff}}{p_S} \approx 1.4 \times \left(\frac{T_0}{T_C}\right)^{\frac{2}{3}} \tag{9}$$

As for Ni_2MnGa, p_{eff} is 4.75 [24,26]. Equation (9) can be rewritten as:

$$k_m = \left(\frac{p_{eff}}{p_S}\right) \times \left(\frac{T_C}{T_0}\right)^{\frac{2}{3}} \tag{10}$$

When k_m is 1.4, Equation (10) is equal to Equation (9). For Ni_2MnGa, a value of 1.61 for k_m was obtained by substituting p_S, T_C, and T_0 from Table 1 and p_{eff} of 4.75 into Equation (10) [26]. The values of k_m for notable atoms, alloys, and compounds are Ni 1.41 [12], MnSi 1.88 [21], Ni_3Al 1.06 [27], $Y(Co_{0.85}Al_{0.15})_2$ 1.08 [28], $ZrZn_2$ 0.74 [29], UCoGe 1.74 [8], and UGe_2 1.61 [8]; these were calculated from the values listed in Table 2. Actinide 5f compound $NpFe_4P_{12}$ was also analyzed using the Takahashi theory and a k_m value of 1.44 was found [30]. Table 2 provides the k_m values and the magnetic moments and characteristic temperatures relating to spin fluctuation. Figure 5 is a plot of $\log(p_{eff}/p_S)$ versus $\log(T_C/T_0)$ for Ni_2MnGa, Ni, and notable alloys and compounds using the data in Table 2. The dotted line indicates the line of Equation (10) when k_m is 1.4. Figure 5 clearly shows that the relation between p_{eff}/p_S and T_o/T_C can be explained by Equation (9). In Figure 3.3. in Takahashi [8], UGe_2 had the largest value of T_C/T_0. In Figure 5 of this article, we added Ni, Ni_2MnGa, and $NpFe_4P_{12}$. The T_C/T_0 value of Ni_2MnGa was almost the same as that of $NpFe_4P_{12}$. The magnetic alloys and compounds that were analyzed by means of Equation (9) under the Takahashi theory were magnets with T_C values lower than room temperature. Notably, the ferromagnetic alloy Ni_2MnGa, which has a T_C higher than room temperature, can be explained by Figure 5 and Equation (6).

Table 2. Basic magnetic parameters and k_m, as obtained from Equation (10).

	T_C (K)	p_{eff} (μ_B)	p_S (μ_B)	p_{eff}/p_S	T_A (K)	T_0 (K)	T_C/T_0	k_m	Reference
Ni_2MnGa	375	4.75 *	3.93	1.21	563	245	1.53	1.61	This work, [26] *
Ni	623	3.3	0.6	5.5	1.76×10^4	4.83×10^3	0.129	1.41	[12]
MnSi	30	2.2	0.4	5.3	2.08×10^3	231	0.13	1.88	[21]
Ni_3Al	41.5	1.3	0.075	17.3	3.09×10^4	3.59×10^3	0.016	1.06	[27]
$Y(Co_{0.85}Al_{0.15})_2$	26	2.15	0.138	15.6	0.726	1.41	0.018	1.08	[28]
$ZrZn_2$	17	1.44	0.12	12	8.83×10^3	321	0.053	0.74	[29]
UCoGe	2.4	1.93	0.039	49.5	5.92×10^3	362	0.0065	1.74	[8]
UGe_2	52.6	3.00	1.41	2.13	442	92.2	0.571	1.61	[8]
$NpFe_4P_{12}$	23	1.55	1.35	1.15	285	16.4	1.40	1.44	[30]

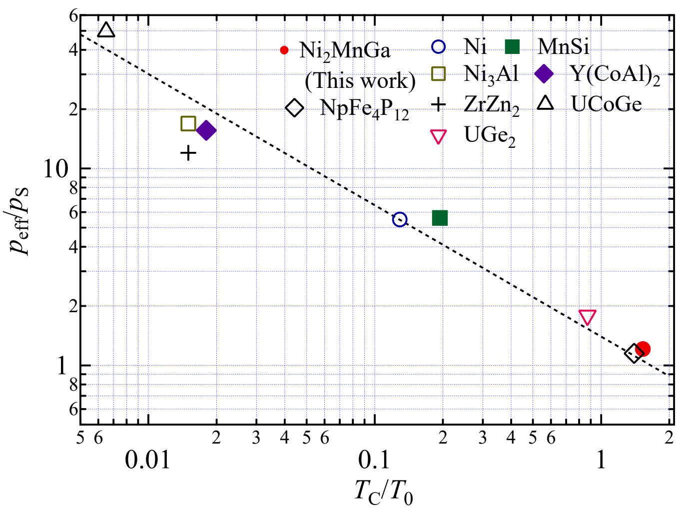

Figure 5. The generalized Rhodes-Wohlfarth plot (double logarithmic plot of p_{eff}/p_S and T_C/T_0) for Ni_2MnGa and other notable alloys and compounds. The dotted line indicates k_m = 1.4 as obtained from Equation (10).

The notable point from Table 2 and Figure 5 is that the p_{eff}/p_S value of Ni_2MnGa is smaller than those of other alloys and compounds. The effective moment p_{eff} was calculated from the Curie constant, $C = N\mu_{eff}^2/3k_B = Np_{eff}^2\mu_B^2/3k_B = N\mu_B^2 p_C(p_C + 2)/3k_B$. The term p_C refers to the effective moment deduced from the Curie constant C. The spontaneous magnetic moment μ is p_S (μ_B) at 0 K. The p_c/p_S was one for local moment ferromagnetism and was larger than one for itinerant ferromagnetism. For Ni_2MnGa, p_{eff} was 4.75, as shown in Table 2; therefore, a p_c value of 3.85 was obtained from the equation $p_{eff}^2 = p_C(p_C + 2)$. Then, the p_C/p_S value was 0.98. As a result, p_C/p_S was a little smaller than one. Webster et al. compared the magnetic moment obtained by saturation magnetization measurement, p_{sat} = 4.17 [26]. Then, p_{sat}/p_S was 0.92. In this work, the magnetization of Ni_2MnGa in the magnetic field of 5.0 T at 5 K was 4.10 μ_B/f.u. Therefore, p_{sat}/p_S was 0.96. The Heusler compounds of CoMnSb and NiMnSb both possess the property of $p_C/p_S < 1$ [31]. Ott et al. proposed a simple molecular field model considering both local moments and spin-polarized itinerant electrons to explain $p_C/p_S < 1$ [31]. They introduced an enhanced temperature-independent

Pauli susceptibility and explained that the Curie constant decreases if the interactions between local magnetic moments and holes is antiferromagnetic. Webster mentioned that in the paramagnetic phase, only the Mn atoms carry a magnetic moment [26]. It is supposed that in the paramagnetic phase, a large moment is induced by the electrons around the Mn atom at the Mn site. Conversely, at the Ni site, the spins fluctuate at high temperature in the paramagnetic phase. Therefore, it is supposed that the magnetic moment p_c at high temperature in a paramagnetic phase is smaller than the spontaneous magnetization p_S and the saturation moment p_{sat} at 5 K.

3.3. Magnetization and Temperature Dependences Force Magnetostrictions

We recorded magnetostriction measurements to conduct an investigation into the magnetization dependence of forced magnetostriction. In our earlier study, the magnetostriction of Ni_2MnGa was found to be proportional to the M^4 of the magnetization and clearly passed through the origin at T_C [14]. In this study, we investigated $Ni_{2+x}MnGa_{1-x}$ (x = 0.02, 0.04) to check whether these relations held when the ratio of Ni to Ga and e/a were varied. We plotted figures of magnetostriction $\Delta L/L$ versus M^δ for δ = 2.0 and 4.0. The result for δ = 2.0 indicates a relation under Moriya's theory [1,15], and that for δ = 4.0 indicates a relation under Takahashi's theory [8]. Figure 6 is a plot of magnetostriction $\Delta L/L$ versus M^2 for x = 0.02 (Figure 6a) and x = 0.04 (Figure 6b). The dotted lines are fitted linear plots. For the magnetostriction at T_C indicated by the filled circles, the M^2 linearity behavior was only observed for large magnetostriction and large magnetization area. Moreover, the dotted straight lines did not pass through the origin. These behaviors are comparable to the results for MnSi [15] and our former result for Ni_2MnGa [13]. We also investigated $\Delta L/L$ versus M^4 dependence, as shown in Figure 7. The plot of $\Delta L/L$ versus M^4 indicates good linearity passing through the origin at T_C, as indicated by the filled circles for both samples. Table 3 provides the coefficients A and k of the fitted linear plots given by the equation $\Delta L/L = A + kM^\delta$ for δ = 2 or 4 at T_C. The standard deviations of the linear fitted lines at T_C for magnetostriction $\Delta L/L$ versus M^2 and $\Delta L/L$ versus M^4 are shown in Figures 6 and 7, respectively, and are also listed in Table 3. The errors of the coefficient k were within $\pm 2\%$ for both values of δ. The proportions of the coefficient A and the magnetostriction at 5 T ($\Delta L/L \simeq -60 \times 10^{-6}$), y_0, were greater than 50% and less than 1.2% for δ = 2 and 4, respectively. This analysis indicates that the magnetostriction can be represented by the equation $\Delta L/L = kM^4$ at T_C, as presented in Figure 7. As a result, the relation between magnetostriction and magnetization confirmed that the magnetostriction is proportional to the fourth power of the magnetization, as derived from Takahashi's theory, even when the ratio of Ni to Ga and e/a were varied.

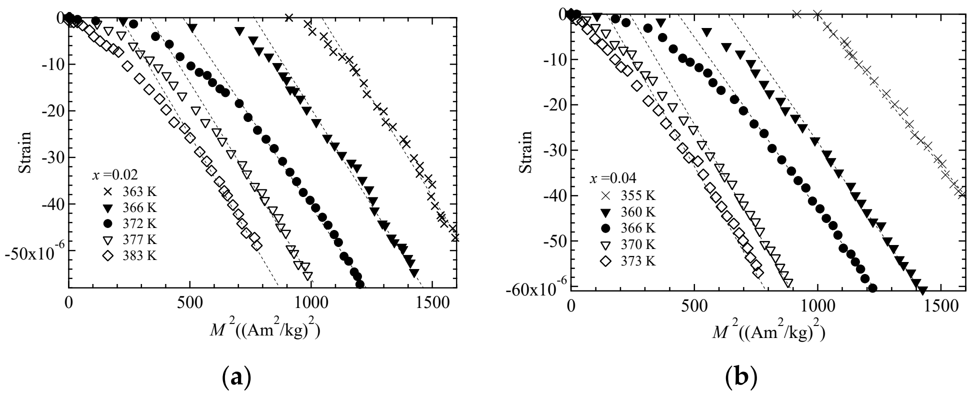

Figure 6. The M^2 dependence of magnetostriction for (**a**) x = 0.02 and (**b**) x = 0.04. The dotted straight lines are included as a visual guide.

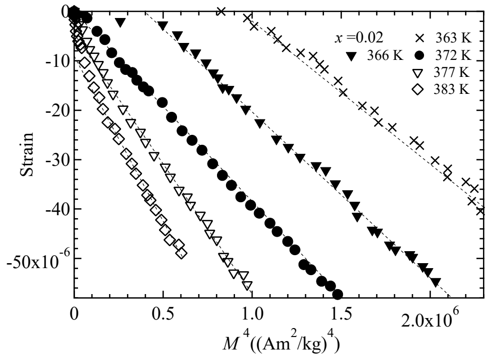

(**a**)

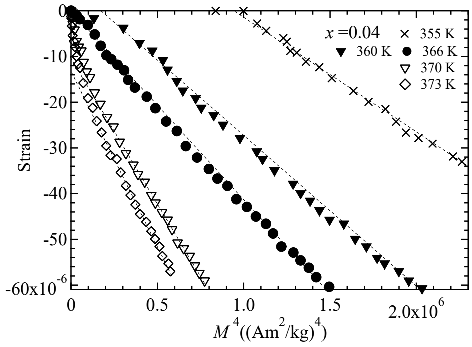

(**b**)

Figure 7. The M^4 dependence of magnetostriction for (**a**) x = 0.02 and (**b**) x = 0.04. The dotted straight lines are included as a visual guide.

Table 3. The coefficients and standard deviations of the linear fitted plots obtained by means of the least squares method at T_C for the magnetostriction $\Delta L/L$ by the equation $\Delta L/L = A + kM^{\delta}$ for δ = 2 or 4, as shown in Figures 5 and 6, respectively. Both A and k are constants.

	$\delta = 2$		$\delta = 4$	
x	0.02	0.04	0.02	0.04
A	3.60×10^{-5}	1.65×10^{-7}	3.29×10^{-5}	-7.06×10^{-7}
Standard deviation of A	$\pm 1.20 \times 10^{-6}$ (3.3% of A)	$\pm 1.73 \times 10^{-7}$ 105% of A)	$\pm 1.04 \times 10^{-6}$ (3.2% of A)	$\pm 2.72 \times 10^{-7}$ (38% of A)
$y_0 = A/$(Strain at 5 T)	58%	0.3%	53%	1.2%
k	-7.62×10^{-8}	-3.93×10^{-11}	-7.58×10^{-8}	-4.11×10^{-11}
Standard deviation of k	$\pm 1.2 \times 10^{-9}$ (1.5% of k)	$\pm 2.08 \times 10^{-13}$ (0.5% of k)	$\pm 1.03 \times 10^{-9}$ (1.4% of k)	$\pm 3.36 \times 10^{-13}$ (0.8% of k)

The magnetostrictions at 5 T were 50×10^{-6}, 58×10^{-6}, and 61×10^{-6} for x = 0.00, 0.02, and 0.04, respectively. With increasing x, the magnetostriction increased. In our former investigation of the magnetostriction of $Ni_2Mn_{1-x}Cr_xGa$ ($x \leq 0.25$), the magnitude of the magnetostriction increased when the premartensite transition temperature T_P and T_C were closer, as shown in Sakon et al. [16]. For $Ni_{2+x}MnGa_{1-x}$, the T_P values were 258 K, 265 K, and 275 K for x = 0.00, 0.02, and 0.04, respectively. The T_C values were 375 K, 372 K, and 366 K for x = 0.00, 0.02, and 0.04, respectively. With increasing x, the T_P shifted to higher temperatures and the T_C shifted to lower temperatures. We supposed that the magnetostriction of $Ni_{2+x}MnGa_{1-x}$ has the same properties as that of $Ni_2Mn_{1-x}Cr_xGa$.

Finally, we discuss the e/a dependences of the maximum magnetostriction around the premartensitic–austenitic transition for Ni_2MnGa-type alloys. Around the premartensitic transition temperature T_P, large magnetostriction has been observed [16,17]. Detailed explanations of the premartensitic transition and premartensite phase have been previously presented [16–18]. In our former investigation [16], we examined the magnetostrictions for $Ni_2Mn_{1-x}Cr_xGa$ (x = 0.00, e/a = 7.50; x = 0.15, e/a = 7.46) around T_P and T_M. With increasing x, T_P and e/a decreased; accordingly, the maximum value of the magnetostriction decreased. We assumed that if e/a increases, T_P and the magnetostriction increase. Matsui et al. experimentally investigated the Ni_2MnGa-type alloys with $e/a > 7.50$ [17,18]. Among these alloys, $Ni_{51.7}Mn_{24.3}Ga_{24.0}$ with T_P = 285 K and e/a = 7.59 showed large magnetostriction with strain 550×10^{-6} [17,18]. In this study, we decided to increase the concentration of Ni and decrease that of Ga because the e/a values of Ni and Ga are 10 and 3, respectively, in order to increase the e/a value of alloys to be above 7.50. Therefore, we prepared $Ni_{2+x}MnGa_{1-x}$ alloys with x = 0.02, producing e/a = 7.535, and x = 0.04, producing e/a = 7.570. Figure 8 shows the temperature dependencies of the magnetostriction at 1.6 T. The values were 250×10^{-6} and 380×10^{-6} for x = 0.02

and 0.04, respectively. Figure 9 shows the e/a dependences of the maximum magnetostriction for Ni_2MnGa-type alloys. The maximum value of magnetostriction was almost proportional to the valence electron concentration per atom, e/a, and we also clarified the correlation between the magnetostriction and the e/a.

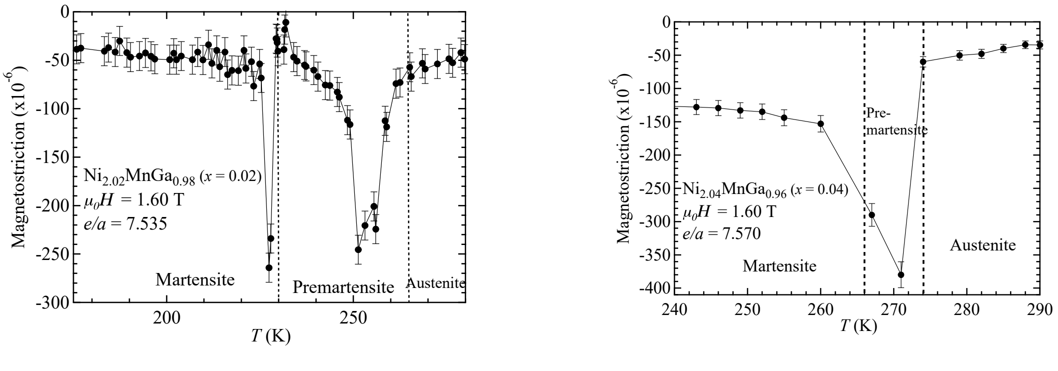

Figure 8. The temperature dependencies of the magnetostriction for (**a**) $x = 0.02$ and (**b**) $x = 0.04$.

The softening of the lattice around T_P was investigated using ultrasonic measurements [32,33]. Seiner et al. investigated the magnetostriction around T_P for a single crystal of Ni_2MnGa [33]. They suggested a model based on adaptive concept of premartensite, explaining the softening of c_{44} and apparent c' stiffening prior to the martensitic transformation and discussed the magneto-elastic coupling effect by means of these magnetostriction, and ultrasonic measurements results under magnetic fields. This consideration only involves the softening of the elastic constant. Our experimental results indicate that the e/a and the magnetostriction are correlated and investigation by means of the itinerant electron magnetism is needed to better understand the fundamental origin of the magnetostriction. Future experimental and fundamental theoretical studies are needed to investigate the magneto-elastic coupling effect precisely, for example, with spectroscopy measurements for investigations of electron band structure and with itinerant electron magnetism theories.

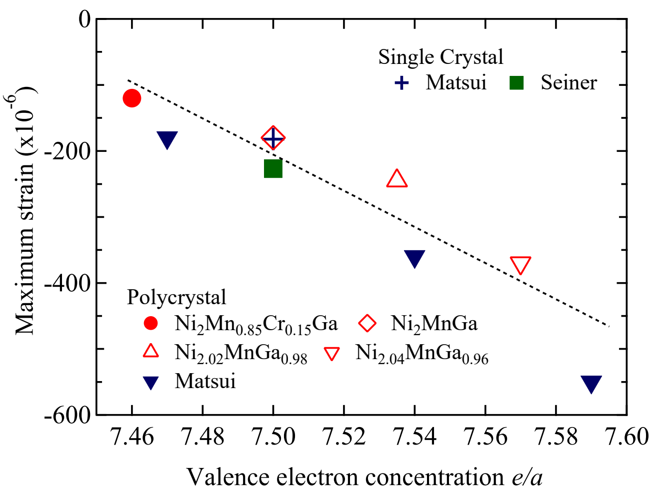

Figure 9. The e/a dependences of the maximum magnetostriction for Ni_2MnGa-type alloys. Filled triangles: polycrystal, Matsui et al. [17,18]. Cross: single crystal, Matsui et al. [17]. Filled square: single crystal, Seiner et al. [33]. The dotted line is a fitted line.

4. Conclusions

Experimental investigations of the field dependence of magnetization and the relationship between magnetization and magnetostriction for $Ni_{2+x}MnGa_{1-x}$ (x = 0.00, 0.02, 0.04) alloy ferromagnets were performed in accordance with the self-consistent renormalization (SCR) spin fluctuation theory of itinerant ferromagnetism. In this study, we investigated the magnetization of and the magnetostriction on $Ni_{2+x}MnGa_{1-x}$ (x = 0.02, 0.04) to check whether these relations held when the ratio of Ni to Ga and e/a were varied. When the ratio of Ni to Ga varied, the valence electron concentration per atom, e/a, increased with increasing x. The magnetization results for x = 0.02 (e/a = 7.535) and 0.04 (e/a = 7.570) suggest that the critical index δ of $H \propto M^{\delta}$ is around 5.0 at the Curie temperature T_C, which is the critical temperature of the ferromagnetic–paramagnetic transition. This result confirms Takahashi's spin fluctuation theory and the experimental results obtained for Ni_2MnGa. The spontaneous magnetization p_S slightly decreased with increasing x. For x = 0.00, the obtained spin fluctuation parameter in k-space (momentum space) T_A and that in energy space T_0 were 563 K and 245 K, respectively. The relationship between p_{eff}/p_S and T_C/T_0 can be explained by Takahashi's theory, where p_{eff} indicates the effective magnetic moments. We produced a generalized Rhodes-Wohlfarth plot of p_{eff}/p_S versus T_C/T_0 values including those of other ferromagnets. The plot indicates that the relation between p_{eff}/p_S and T_0/T_C follows Takahashi's theory. We also measured the magnetostriction for $Ni_{2+x}MnGa_{1-x}$ (x = 0.02, 0.04). At T_C, the plot of the magnetostriction $\Delta L/L$ versus M^4 showed proportionality and crossed the origin. These magnetization and magnetostriction results were analyzed in the context of Takahashi's SCR spin fluctuation theory. Further, we investigated the magnetostriction at the premartensite phase, which is the precursor state to the martensitic transition. In Ni_2MnGa system alloys, the maximum value of magnetostriction is almost proportional to e/a.

Author Contributions: Sample preparation, D.L., F.H., G.O., T.E.; magnet system preparation, T.S., Y.H., Y.N., M.H.; investigation, T.S., T.E., Y.H., Y.N., M.H.; writing—original draft preparation, T.S, Y.H., T.E.; writing—review and editing, T.S., T.K.; supervision, T.K.

Funding: This research was founded by Visiting Researcher's Program of the Institute for Solid State Physics, the University of Tokyo.

Acknowledgments: The authors thank Mitsuo Kataoka for helpful discussions. The authors also thank Mitsuo Okamoto and Fumihiko Morioka of Ryukoku University for helping to create the apparatus. This project is partly supported by the Ryukoku Extension Center (REC) at Ryukoku University. This research was carried out in part at the International Research Center for Nuclear Materials Science, Institute for Materials Research, Tohoku University. This research was also carried out at the Center for Advanced High Magnetic Field Science in Osaka University under the Visiting Researcher's Program of the Institute for Solid State Physics, the University of Tokyo.

Conflicts of Interest: The authors declare no conflict of interest.

References

1. Moriya, T. *Spin Fluctuations in Itinerant Electron Magnetism*; Springer: Berlin, Germany, 1985; ISBN 978-3-642-82499-9.
2. Lonzarich, G.; Taillefer, G. Effect of spin fluctuations on the magnetic equation of state of ferromagnetic or nearly ferromagnetic metals. *J. Phys. C Solid State Phys.* **1985**, *18*. [CrossRef]
3. Takahashi, Y. On the origin of the Curie Weiss law of the magnetic susceptibility in itinerant electron magnetism. *J. Phys. Soc. Jpn.* **1986**, *55*. [CrossRef]
4. Takahashi, Y. Theoretical Development in Itinerant Electron Ferromagnetism. *J. Phys. Conf. Ser.* **2017**. [CrossRef]
5. Takahashi, Y.; Nakano, H. Magnetovolume Effect of Itinerant Electron Magnetism. *J. Phys. Condens. Matter* **2006**, *18*. [CrossRef]
6. Moriya, T.; Kawabata, A. Effect of Spin Fluctuations on Itinerant Electron Ferromagnetism. *J. Phys. Soc. Jpn.* **1973**, *34*. [CrossRef]
7. Moriya, T.; Kawabata, A. Effect of Spin Fluctuations on Itinerant Electron Ferromagnetism. II. *J. Phys. Soc. Jpn.* **1973**, *35*. [CrossRef]

8. Takahashi, Y. *Spin Fluctuation Theory of Itinerant Electron Magnetism*; Springer: Berlin, Germany, 2013; ISBN 978-3-642-36666-6.
9. Rhodes, P.; Wohlfarth, E.P. The effective Curie-Weiss constant of ferromagnetic metals and alloys. *Proc. R. Soc. Lond. A* **1963**, *273*. [CrossRef]
10. Nishihara, H.; Harada, T.; Kanomata, T.; Wada, T. Magnetizationprocess near the Curie temperature of an itinerant ferromagnet CoS_2. *J. Phys. Conf. Ser.* **2012**, *400*, 032068. [CrossRef]
11. Shimizu, K.; Maruyama, H.; Yamazaki, H.; Watanabe, H. Effect of Spin Fluctuations on Magnetic Properties and Thermal Expansion in Pseudobinary System $Fe_xCo_{1-x}Si$. *J. Phys. Soc. Jpn.* **1990**, *59*. [CrossRef]
12. Nishihara, H.; Komiyama, K.; Oguro, I.; Kanomata, T.; Chernenko, V. Magnetization processes near the Curie temperatures of the itinerant ferromagnets, Ni_2MnGa and pure nickel. *J. Alloys Compd.* **2007**, *442*, 191–193. [CrossRef]
13. Sakon, T.; Hayashi, Y.; Fujimoto, N.; Kanomata, T.; Nojiri, H.; Adachi, Y. Forced magnetostriction of ferromagnetic Heusler alloy Ni_2MnGa at the Curie temperature. *J. Appl. Phys.* **2018**, *123*. [CrossRef]
14. Kittel, C. *Introduction of Solid State Physics*, 8th ed.; John Wiley & Sons Inc.: Hoboken, NJ, USA, 2004; p. 75. ISBN 978-0-471-41526-8.
15. Matsunaga, M.; Ishikawa, Y.; Nakajima, T. Magneto-volume effect in the weak itinerant ferromagnet MnSi. *J. Phys. Soc. Jpn.* **1982**, *51*. [CrossRef]
16. Sakon, T.; Fujimoto, N.; Kanomata, T.; Adachi, Y. Magnetostriction of $Ni_2Mn_{1-x}Cr_xGa$ Heusler alloys. *Metals* **2017**, *7*, 410. [CrossRef]
17. Matsui, M.; Nakakura, T.; Murakami, D.; Asano, H. Super magnetostriction with mesophase transition of Ni_2MnGa. *Toyota Sci. Rep.* **2010**, *63*, 27–36.
18. Matsui, M.; Nakamura, T.; Murakami, D.; Yoshimura, S.; Asano, H. Effect of Super Magnetostriction on Magnetic Anisotropy of Ni_2MnGa. *Toyota Sci. Rep.* **2011**, *64*, 1–11.
19. Rizal, C.; Kolthammer, J.; Pokharel, R.K.; Choi, B.C. Magnetic properties of nanostructured Fe-Co alloys. *J. Appl. Phys.* **2013**, *113*. [CrossRef]
20. Singh, S.; Bednarcik, J.; Barman, S.R.; Felsher, S.R.; Pandey, D. Premartensite to martensite transition and its implications for the origin of modulation in Ni_2MnGa ferromagnetic shape-memory alloy. *Phys. Rev. B* **2015**, *92*. [CrossRef]
21. Bloch, D.; Voiron, J.; Jaccarino, V.; Wernick, J.H. The high field-high pressure magnetic properties of MnSi. *Phys. Lett. A* **1975**, *51*, 259–261. [CrossRef]
22. Hatta, S.; Chikazumi, S. Magnetization Process in High Magnetic Fields for Fe and Ni in Their Critical Regions. *J. Phys. Soc. Jpn.* **1977**, *43*, 822–830. [CrossRef]
23. Tanaka, Y.; Ishida, S.; Asano, S. Band Calculation of Manganese Magnetic Moments in Ni_2MnGa 14M Structure. *Mater. Trans. JIM* **2004**, *45*, 1060–1064. [CrossRef]
24. Khovailo, V.V.; Novosad, V.; Takagi, T.; Filippov, D.A.; Levitin, R.Z.; Vasil'ev, A.N. Magnetic properties and magnetostructural phase transitions in $Ni_{2+x}Mn_{1-x}Ga$ shape memory alloys. *Phys. Rev. B* **2004**, *70*. [CrossRef]
25. Ueda, U.; Takahashi, M. Structure and Magnetic Properties of Electrodeposited Fe-Ni Alloy Films. *J. Phys. Soc. Jpn.* **1980**, *49*, 477–483. [CrossRef]
26. Webster, P.J.; Ziebeck, K.R.A.; Town, S.L.; Peak, M.S. Magnetic order and phase transformation in Ni_2MnGa. *Philos. Mag. B* **1984**, *49*, 295–310. [CrossRef]
27. De Boer, F.R.; Biesterbos, J.; Schinkel, C.J. Ferromagnetism in the intermetallic phase Ni_3Al. *Phys. Lett. A* **1969**, *24*, 355–357. [CrossRef]
28. Yoshimura, K.; Takigawa, M.; Takahashi, Y.; Yasuoka, H.; Nakamura, Y. NMR Study of Weakly Itinerant Ferromagnetic $Y(Co_{1-x}Al_x)_2$. *J. Phys. Soc. Jpn.* **1987**, *56*, 1138–1155. [CrossRef]
29. Ogawa, S. Electrical Resistivity of Weak Itinerant Ferromagnet $ZrZn_2$. *J. Phys. Soc. Jpn.* **1976**, *40*, 1007–1009. [CrossRef]
30. Aoki, D.; Haga, Y.; Homma, Y.; Sakai, H.; Ikeda, S.; Shiokawa, Y.; Yamamoto, E.; Nakamura, A.; Onuki, Y. First single crystal growth of the Transuranium filled-Skutterudite compound $NpFe_4P_{12}$ and its magnetic and electrical properties. *J. Phys. Soc. Jpn.* **2006**, *75*. [CrossRef]
31. Otto, M.J.; van Woerden, R.A.M.; van der Valk, P.J.; Wijngaard, J.; van Bruggen, C.F.; Haas, C.; Buschow, K.H.J. Half-metallic ferromagnets. I. Structure and magnetic properties of NiMnSb and related inter-metallic compounds. *J. Phys. Condens. Matter* **1989**, *1*, 2341–2350. [CrossRef]

32. Mejía, C.S.; Born, N.O.; Schiemer, J.A.; Felser, C.; Carpenter, M.A.; Nicklas, M. Strain and order-parameter coupling in Ni-Mn-Ga Heusler alloys from resonant ultrasound spectroscopy. *Phys. Rev. B* **2018**, *97*, 094410. [CrossRef]
33. Seiner, H.; Kopecky, V.; Landa, M.; Heczko, O. Elasticity and magnetism of Ni_2MnGa premartensitic tweed. *Phys. Status Solidi B* **2014**, *251*, 2097–2103. [CrossRef]